Diagnostic and Prognostic Value of microRNAs for Environmental Exposure to Asbestiform Fibers Causing the Malignant Mesothelioma

Veronica Filetti
University of Catania
Carla Loreto
University of Catania
Luca Falzone
University of Catania
Claudia L Lombardo
University Of Catania
Emanuele Cannizzaro
University of Palermo: Universita degli Studi di Palermo
Sergio Castorina
University of Catania
Caterina Ledda (cledda@unict.it)
Universita degli Studi di Catania https://orcid.org/0000-0003-0739-8798
Venerando Rapisarda
University of Catania

Research

Keywords: Fluoro-edenite, Asbestos, Malignant Mesothelioma, microRNA, Diagnosis, Prognosis

Posted Date: May 5th, 2021

DOI: https://doi.org/10.21203/rs.3.rs-448056/v1

Abstract

Background

Fluoro-edenite (FE) is an asbestiform fiber identified in the lavic products of Monte Calvario from stone quarries located in the southeast of Biancavilla (Sicily, Italy). Environmental exposure to this silicate has been associated with a higher incidence of Malignant Mesothelioma (MM), highly aggressive cancer that affects the pleural tissue. Median survival for MM was 9.8 months, with 5% of patients surviving at 5 years. At present, several diagnostic biomarkers have been evaluated for MM and many studies demonstrated that microRNAs (miRNAs) have the potential to be considered as good non-invasive diagnostic and prognostic biomarkers for cancer.

A set of miRNAs involved in MM was previously identified after a careful *in silico* selection. Starting from these preliminary data, this study aimed to validate the predicted diagnostic significance of hsa-miR-323a-3p, hsa-miR-101-3p, and hsa-miR-20b-5p on a subset of MM patients exposed to FE and matched healthy controls. For this purpose, MM tissues *vs.* nonmalignant pleura tissues were analyzed through droplet digital PCR to evaluate differences in the expression levels of these miRNAs and their MM diagnostic potential. In addition, computational analysis have been performed to establish the correlation of these miRNAs with the online available asbestos exposure data and clinic-pathological parameters to verify a potential role of these miRNAs as prognostic tools. The interaction between these miRNAs and the main genes mutated and altered in MM was evaluated.

Results

Droplet digital PCR results showed that the three analyzed miRNAs were significantly down-regulated in MM cases *vs.* controls. ROC analysis revealed high specificity and sensitivity rates for both hsa-miR-323a-3p, and hsa-miR-20b-5p, which thus acquire a diagnostic value for MM. *In silico* results showed a potential prognostic role of hsa-miR-101-3p due to a significant association of its higher expression and increased Overall Survivor of MM patients. Finally, the computational analysis have showed that these miRNAs can target and modulate both oncogene and tumor suppressor genes.

Conclusions

These miRNAs should be further evaluated not only as diagnostic tools, but also as prognostic predictors. Furthermore, the validation of their targets and regulators would clarify how miRNAs induce or repress critical pathways involved in the carcinogenesis triggered by carcinogenic fibers exposure.

Background

The types of minerals forming fibers that have been used commercially and that are known with the term “asbestos” include the serpentine (chrysotile) and the fibrous amphiboles cummingtonite-grunerite (amosite asbestos), actinolite, anthophyllite, riebeckite (crocidolite asbestos), anthracite, and tremolite [1,

2]. Such fibers represent an environmental health problem as chronic exposure to these minerals has been associated with respiratory diseases, including cancer.

Additionally, exposure to several other types of mineral particles found in the natural environment and termed “naturally occurring asbestos” (NOA) such as fibers of the minerals erionite, winchite, magnesio-riebeckite, Libby asbestos, richterite, antigorite, and fluoro-edenite (FE), have also been associated with Malignant Mesothelioma (MM) [1, 2].

FE is a calcium amphibole of transparent and intense yellow colour [3]. This silicate has several properties similar to the asbestos group [4, 5]; in particular, it presents the same morphological and compositional aspect of the two fibrous phases tremolite and actinolite [2]. However, the peculiar feature of Biancavilla FE is its composition characterized by high aluminum, fluorine, and sodium contents, compared with other known oncogenic minerals [6].

The International Agency of Research on Cancer (IARC) classified the FE fibers as carcinogenic to humans [7]. FE fibers effects similar to those already reported after the exposure to asbestos fibers have been shown by several epidemiological studies [8, 9, 10, 11, 12, 13, 14, 15]. Indeed, several studies have reported an increased incidence of malignant neoplasms affecting the pleura, the peritoneum, and the lung, after the chronic inhalation of FE fibers [16, 17, 18]. All data suggest that the FE fibers exposure is caused to environmental contamination and it is not due to specific occupational tasks [16]. The environmental exposure estimate is responsible for 10.8% of MM cases in Italy [19]. The material from the quarry of Monte Calvario (Biancavilla, Italy) has been used for about 50 years for local construction [8, 10, 20], and none of the residents diagnosed for MM had been significantly exposed to asbestos during their occupational activities [21].

The local inflammation in the lung and pleura is among the most recognized toxic effects of FE fibers exposure predisposing the individuals to the MM development [22, 23]. At present, MM has still considered a lethal cancer today characterized by a considerable period of latency (≥ 30–60 years) [24], a late diagnosis that determines poor prognosis and quality of life, and unresponsiveness to currently available treatments [25]. To date, there are no diagnostic tools with high sensitivity and specificity that can be used to perform an early diagnosis of MM in asymptomatic people. Many biomarkers have been proposed for the screening and diagnosis of MM in exposed subjects [26, 27, 28, 29, 30]. The only Food and Drug Administration (FDA)-approved biomarker for MM is the mesothelin [31, 32, 33], but its poor sensitivity limits the diagnosis of MM [34]. Furthermore, recent studies demonstrated that microRNAs (miRNAs) play an important role in MM biology and they have the potential to be considered as good non-invasive diagnostic and prognostic biomarkers and therapeutic targets for cancer [35, 36, 37]. In particular, Micolucci and colleagues [38] propose an early diagnosis of MM or a tool to monitor the therapy sensitivity through the expression levels analysis of several MM-associated miRNAs designated as “mesomiRs” [38]. The goal of this study was to evaluate the expression levels of a set of miRNAs previously identified and already validated in *in vitro* MM model [39] in order to validate their potential use as diagnostic biomarkers for MM. In this study, for the first time, hsa-miR-323a-3p, hsa-miR-101-3p, and

hsa-miR-20b-5p has been analyzed in "*ex vivo*" MM tissues *vs.* nonmalignant pleura tissues. Furthermore, an *in silico* analysis has been performed to evaluate the prognostic and therapeutic role of these three miRNAs. With this research work, we would contribute to basic biomarkers research, and we hope to transfer these results to clinical practice.

Results

Evaluation of miRNA expression profiling using droplet digital PCR

The expression of hsa-miR-323a-3p, hsa-miR-101-3p, hsa-miR-20b-5p was examined in MM tissues and relative controls of healthy pleural mesothelium.

Shapiro-Wilk Normality test showed that the expression levels of the three miRNAs analyzed in MM cases and healthy controls differs significantly from a normal distribution.

The comparison between tumor and normal tissues showed a different expression of the three miRNAs analyzed in MM and healthy controls. The expression levels of hsa-miR-323a-3p, hsa-miR-101-3p and hsa-miR-20b-5p in MM cases were significantly lower compared to controls (Fig. 1). There was a statistically significant trend of down-regulation observed for the three selected miRNAs analyzed in MM cases *vs.* controls.

To assess the sensitivity and specificity of these miRNAs and their role as novel promising diagnostic biomarkers for MM, ROC (Receiver Operating Characteristic) curves were calculated (Fig. 2). ROC analysis revealed high specificity and sensitivity rates for both hsa-miR-323a-3p and hsa-miR-20b-5p. In particular, the sensitivity and specificity for hsa-miR-323a-3p and hsa-miR-20b-5p were 100% and 100% [AUC (Area Under the Curve) = 1]. For hsa-miR-101-3p the sensitivity was 100% and the specificity was 40% (AUC = 0.8625). However, the AUCs of all analyzed miRNAs were statistically significant ($P < 0.05$).

In silico interaction between miRNAs and main genes involved in malignant mesothelioma

Gene target analysis performed by the bioinformatics tool microRNA Data Integration Portal (mirDIP) showed the level of interaction of the three computationally identified miRNAs with the main altered or mutated gene in MM.

We take into account 20 different genes obtained from the Catalogue Of Somatic Mutation In Cancer (COSMIC) and the mirDIP analysis revealed that the three evaluated miRNAs were able to interact with all genes involved in MM with high levels of intensity. These genes were: BAP1 (24%), NF2 (18%), TP53 (12%), SETD2 (7%), LATS2 (5%), FBXW7 (2%), DDX3X (3%), EGFR (1%), SF3B1 (2%), PBRM1 (2%), KRAS (1%), PIK3CA (1%), CTNNB1 (1%), CREBBP (2%), NSD1 (2%), ZFHX3 (2%), APC (1%), LATS1 (2%), LRP1B (2%), BRAF (1%). In particular, for each miRNA were reported the intensity of interaction, from medium to very high specificity. All miRNAs showed very high and high interaction levels with at least 50% of the genes analyzed suggesting a potential role of these miRNAs in the development of MM. According to this analysis, hsa-miR-20b-5p showed very high and high interaction levels with the 85% of the genes mutated

in MM. The genes linked with higher levels of intensity by miRNAs were found to be PBRM1 and ZFHX3, which showed in all cases very high levels of interaction. Also, the KRAS gene showed very high levels of interaction with hsa-miR-323a-3p, hsa-miR-20b-5p, and high levels of interaction with hsa-miR-101-3p. In opposition, the genes associated with medium levels of intensity by all miRNAs were found to be BAP1 and BRAF. None of the genes analyzed showed low levels of interaction intensity with the miRNAs evaluated (Fig. 3).

According to this analysis, these three miRNAs can target and modulate both tumor suppressor and oncogene genes playing a potentially key role in tumor cell development.

In silico interaction between miRNAs and asbestos exposure, tumor stage, and patient survival

Shapiro-Wilk Normality test showed that the expression levels of the three miRNAs contained in the TCGA - MESO database have a normal distribution.

The analysis of miRNAs expression levels according to the asbestos exposure data contained in the TCGA - MESO database revealed that the expression levels of hsa-miR-323a-3p, hsa-miR-101-3p and hsa-miR-20b-5p did not change significantly in MM patients exposed and non exposed to asbestos fibers (Fig. 4).

The analysis of miRNAs expression levels according to the clinical-pathological data contained in the TCGA - MESO database showed that the expression levels of hsa-miR-323a-3p, hsa-miR-101-3p and hsa-miR-20b-5p did not change significantly in MM patients with different tumor stages (Fig. 5).

Finally, considering the median Overall Survival (OS), the Disease – Specific Survival (DSS) and the Progression – Free Interval (PFI) between high and low miRNAs expression, has been showed a significance for the hsa-miR-101-3p ($P < 0.0001$). In particular, there was an association of high hsa-miR-101-3p expression and increased OS Time (Fig. 6A), DSS Time (Fig. 6B), and PFI Time (Fig. 6C). On the contrary, hsa-miR-323a-3p and hsa-miR-20b-5p did not show significant results in MM patients' survival.

Discussion

In this study, for the first time, hsa-miR-323a-3p, hsa-miR-101-3p, hsa-miR-20b-5p have been analyzed in MM tissues *vs.* nonmalignant pleura tissues. All tested miRNAs in MM tissue showed a down-regulation compared to controls.

These translational data about hsa-miR-101-3p obtained in the present study were totally in accordance with our previous research work that showed a significant down-regulation in MM samples compared to controls (Filetti et al., 2020b). Furthermore, this miRNA showed a prognostic value for MM because our new *in silico* results demonstrated a significant association of higher hsa-miR-101-3p expression and increased OS.

Noteworthy, the results obtained for hsa-miR-323a-3p and hsa-miR-20b-5p were opposite to those obtained in our previous *in silico* and *in vitro* analysis, however, for these miRNAs ROC analysis revealed high sensitivity and specificity in correctly distinguishing MM and normal samples.

The computational analysis performed to further establish the functional role of these three miRNAs in MM pathogenesis have showed that these miRNAs can target and modulate both tumor suppressor and oncogene genes playing a potentially key role in tumor cell development.

Several studies have tried to identify novel diagnostic biomarkers for the management of MM patients, however, the currently available diagnostic strategies, mainly based on the evaluation of tumor biomarkers such as Calretinin, Cytokeratin 5, Podoplanin, Mesothelin, Osteopontin, Hyaluronic Acid, Fibulin-3 [26], Vascular Endothelium Growth Factor [27], Acquaporin-1 [28], High Mobility Group Box 1 [29], MacroH2A.1 [30], often fail to diagnose correctly MM due to the low rates of sensitivity and specificity of these biomarkers.

To date, liquid biopsy is emerging as a helpful tool for non-invasive diagnosis, screening, prognosis, stratification of cancer patients [40, 41, 42], and to characterize tumor heterogeneity [43]. The literature already proposes an early diagnosis of MM through the expression levels analysis of several “mesomiRs” [38]. Circulating miRNA-126-3p, miRNA-625-3p, miRNA-103a-3p in blood in pairing with Mesothelin and Fibulin-3 have been suggested as potential diagnostic biomarkers of MM [38]. This approach could avoid the histopathological and immunohistochemistry techniques used as the standard for the late diagnosis of pleural biopsies [19]. It could be particularly helpful to study and subsequently use a combination of several protein and molecular markers to improve diagnostic accuracy.

For this purpose, droplet digital PCR (ddPCR) investigations as well as *in silico* analysis have been performed to assess the functional role of the selected miRNAs and their predictive value for MM patients’ diagnosis and prognosis.

Our results indicated that by increasing the number of samples these miRNAs should be further evaluated not only as diagnostic tools, but also as prognostic predictors. Thus, their potential as therapeutic targets could be explored by assessing their molecular role. Another key task is the validation of their targets and regulators, which would clarify how miRNAs induce or repress critical pathways involved in the carcinogenesis triggered by carcinogenic fibers exposure.

Conclusions

Early detection of circulating tumor biomarkers and tumor DNA represents one of the most promising strategies to improve the survival of cancer patients by increasing treatment efficiency [42, 43, 44]. After this preliminary “*ex vivo*” data, further studies will be designed for the validation of “mesomiRs” with diagnostic potential, alone or in combination with other protein biomarkers, to test their clinical role in high-risk individuals. Certainly, a limitation of the work is the low number of samples available. It would also be interesting to have available a cohort of subjects exposed to FE fibers but in the absence of

tumors. This comparison could highlight any similarities or epigenetic differences not only between oncological subjects and not, but also between those exposed to carcinogenic fibers and not. Moreover, further basic research work should be aimed to investigate the molecular pathways that are regulated by aberrantly expressed miRNAs.

A fundamental future objective is the validation of these results in a subset of patients chronically exposed to FE using the liquid biopsy, to provide a minimally invasive screening tool for the secondary prevention of MM.

Methods

Patients and samples collection

Tissue specimens of ten cases of malignant mesothelioma and four cases of healthy pleural mesothelium were retrospectively analyzed. Formalin-fixed and paraffin-embedded (FFPE) tissue specimens were obtained from the biobank of the Section of Anatomic Pathology, Department Gian Filippo Ingrassia, University of Catania. The exclusion criteria adopted in the choice of the cases were the following: (i) it was not possible to obtain additional slides from FFPE blocks for the analysis; (ii) no representative neoplastic tissue was contained in FFPE blocks. No written informed consent was necessary because the retrospective nature of the study; the research protocols were conformed to the ethical guidelines of the Helsinki Declaration.

The cohort of patients of Biancavilla with FE-mediated MM was composed of six men and four women (mean age: 68.4 ± 13.9 years; age range: 50–93 years). According to the World Health Organization (WHO) criteria, six cases were histologically classified as epithelioid, three were classified as biphasic subtypes, and one was classified as sarcomatoid [19]. The cohort of control cases was composed of eight men (mean age: 44 ± 25.5 years; age range: 15–76 years). These patients did not live in Biancavilla, and they did not show oncological pathologies but pulmonary emphysema (n = 3) and pleurisy (n = 5). Data including MM cases and controls are summarized in Table 1.

Freshly cut sections of FFPE tissue, each with a thickness of 20 μm, were obtained by a rotary microtome. Two sections for each sample have been collected and stored at room temperature.

Table 1
Features of the fluoro-edenite (FE)-related malignant mesothelioma (MM) cases and controls.

	Age range (Years)	Mean age (Years)	Gender	Pathologies	Pathological Subtype	Survival Time range (Days)	Mean Survival Time (Days)
Cases (N = 10)	50–93	68.4 ± 13.9	60% men, 40% women	100% malignant mesothelioma	60% epithelioid, 10% sarcomatoid, 30% biphasic	45–1800	579 ± 525
Controls (N = 8)	15–76	44 ± 25.5	100% men	37.5% pulmonary emphysema, 62.5% pleurisy			

RNA isolation and RT

Total RNA containing small non-coding RNA was extracted from FFPE tissue using miRNeasy FFPE Kit (QIAGEN; Hilden, Germany) according to the manufacturer's recommended protocol (miRNeasy FFPE Handbook 01/2020). The RNA extraction and quantification were performed as previously described [39]. All samples were then stored at -80°C until use. The purified RNA was reverse transcribed into cDNA as previously described [39].

Droplet Digital PCR

As previously described, a customized ddPCR assay was used to amplify hsa-miR-323a-3p, hsa-miR-101-3p, and hsa-miR-20b-5p [45]. The reaction mixture was prepared by adding the ddPCR Supermix for probes (no dUTP) (cat. n. 1863010 – Bio-Rad Laboratories), the TaqMan Advanced miRNA Assays specific for each miRNA (cat. n. 477863, 477804, 477853 - Thermo Fisher Scientific), the miR-Amp cDNA sample and the PCR water. The cartridge was loaded with 20 microliters of PCR reaction and 70 µL of Droplet Generation Oil (cat. n. 1863005 - Bio-Rad Laboratories) in appropriate wells, and then Droplet Generator QX200 was used to generate droplets. Subsequently, the generated droplets were amplified by using C 1000 Touch Thermal Cycler (Bio-Rad Laboratories) at the cycling conditions previously described [39]. A Non-Template Control (NTC) has been inserted for each probe.

After the amplification, the droplets were read by QX200 Droplet Reader (Bio-Rad Laboratories). Finally, the absolute quantification of targets was calculated by using the QuantaSoft software, version 1.7.4 (QuantaSoft, Prague, Czech Republic), as previously described [39, 46].

In silico analysis

To clarify the role of hsa-miR-323a-3p, hsa-miR-101-3p and hsa-miR-20b-5p in MM, different computational models have been used.

By consulting the COSMIC (http://cancer.sanger.ac.uk/cosmic) it was possible to identify the 20 most mutated genes that are known to be involved in MM development and therefore have a dysregulated expression. The selection was performed using the search term “Malignant Mesothelioma” including the terms “Pleura” in tissue selection and “Mesothelioma” in histology selection.

Subsequently, using the bioinformatics prediction tool mirDIP version 4.1.11.2, Database version 4.1.0.3, Nov 2020) (http://ophid.utoronto.ca/mirDIP) [47, 48], the interaction between the miRNA previously identified by computational analysis and the main genes mutated and altered in MM was evaluated.

Furthermore, the clinical implication of the three analyzed miRNAs was assessed through the clinic-pathological data and the miRNA expression profiles analysis contained in The Cancer Genome Atlas - Mesothelioma (TCGA - MESO) database and downloaded by using the online exploration tool UCSC Xena Browser (https://xenabrowser.net/) [49]. In particular, the TCGA database has been used to verify if the three miRNAs we analyzed were dysregulated in MM according to asbestos exposure, tumor stage, and patient survival. A total of 17 MM patient-related datasets were found with a total of 87 MM samples (35 exposed to asbestos, 49 not exposed to asbestos, 3 excluded due to lack of useful information). The datasets contained the expression levels of 1,964 different miRNAs, but we focused on the hsa-miR-323a-3p, hsa-miR-101-3p and hsa-miR-20b-5p for further investigation.

Statistical analysis

The Shapiro-Wilk Normality test was used for the calculation of the distribution of hsa-miR-323a-3p, hsa-miR-101-3p and hsa-miR-20b-5p expression levels observed with ddPCR and deposited on the TCGA - MESO database. The Mann-Whitney test was used for the comparison between miRNAs expression of MM samples and healthy controls. ROC curves were obtained to evaluate the specificity and sensitivity of the analyzed miRNAs. One-way ANOVA test and unpaired Student t-test were used for assessing the statistical differences existing between the expression levels of hsa-miR-323a-3p, hsa-miR-101-3p and hsa-miR-20b-5p reported in the TCGA - MESO database according to the MM tumor stages and the asbestos exposure, respectively. Cancer-specific survival analysis was performed using the Kaplan-Meier method, and for comparison of the survival curves, the Mantel-Cox log-rank test was used.

A value of $P < 0.05$ was considered statistically significant. The data were plotted using Prism for Windows version 7.00 (Graphpad Software; CA, USA).

Abbreviations

FE: Fluoro-edenite

MM: Malignant Mesothelioma

miRNAs: microRNAs

ddPCR: droplet digital PCR

NOA: naturally occurring asbestos

IARC: International Agency of Research on Cancer

FDA: Food and Drug Administration

ROC: Receiver Operating Characteristic

AUC: Area Under the Curve

OS: Overall Survival (OS)

DSS: Disease – Specific Survival (DSS)

PFI: Progression – Free Interval

FFPE: Formalin-fixed and paraffin-embedded

WHO: World Health Organization

NTC: Non-Template Control

COSMIC: Catalogue Of Somatic Mutation In Cancer

mirDIP: microRNA Data Integration Portal

TCGA – MESO: The Cancer Genome Atlas - Mesothelioma

Declarations

Ethics approval and consent to participate

Not applicable.

Consent for publication

All authors have read and approved the manuscript. The need for publication is not applicable.

Availability of data and materials

The data are available from the corresponding author on reasonable request.

Competing interests

The authors declare that they have no competing interest.

Funding

This research did not receive any specific grant from funding agencies in the public, commercial, or not-for-profit sectors.

Authors' contributions

Veronica Filetti: Conceptualization, Data Curation, Formal Analysis, Investigation, Methodology, Project administration, Software, Validation, Visualization, Roles/Writing - original draft, Writing - review & editing; Carla Loreto: Conceptualization, Funding acquisition, Resources, Visualization, Supervision, Writing - review & editing; Luca Falzone: Conceptualization, Data Curation, Formal Analysis, Investigation, Methodology, Software, Validation, Visualization, Writing - review & editing; Claudia Lombardo: Visualization, Supervision; Emanuele Cannizzaro: Visualization, Supervision; Sergio Castorina: Visualization, Supervision; Caterina Ledda: Conceptualization, Funding acquisition, Resources, Visualization, Supervision; Venerando Rapisarda: Conceptualization, Funding acquisition, Resources, Visualization, Supervision.

Acknowledgements

Not applicable.

References

1. Baumann F, Ambrosi J-P, Carbone M. Asbestos is not just asbestos: an unrecognised health hazard. Lancet Oncol. 2013;14:576–578.
2. Filetti V, Vitale E, Broggi G, Hagnäs MP, Candido S, Spina A, Lombardo C. Update of *in vitro*, *in vivo* and *ex vivo* fluoro-edenite effects on malignant mesothelioma: A systematic review (Review). Biomedical Reports. 2020;00(BR-12723-251879_Filetti , 0000).
3. Soffritti M, Minardi F, Bua L, Degli Esposti D, Belpoggi F. First experimental evidence of peritoneal and pleural mesotheliomas induced by fluoro-edenite fibres present in Etnean volcanic material from Biancavilla (Sicily, Italy). Eur J Oncol. 2004;9(3):169-175.
4. Comba P, Gianfagna A, Paoletti L. Pleural mesothelioma cases in Biancavilla are related to a new fluoro-edenite fibrous amphibole. Arch. Environ. Health. 2003;58:229-232.
5. Biggeri A, Pasetto R, Belli S, Bruno C, Di Maria G, Mastrantonio M, Trinca S, Uccelli R, Comba P. Mortality from chronic obstructive pulmonary disease and pleural mesothelioma in an area contamined by natural fibre (fluoro-edenite). Scand J Work Environ Health. 2004;30:249-252.
6. Gianfagna A, Ballirano P, Bellatreccia F, Bruni B, Paoletti L, Oberti R. Characterization of amphibole fibres linked to mesothelioma in the area of Biancavilla, Eastern Sicily, Italy. Mineralogical Magazine. 2003;67:1221-1229.
7. Grosse Y, Loomis D, Guyton KZ, Lauby-Secretan B, El Ghissassi F, Bouvard V, Benbrahim-Tallaa L, Guha N, Scoccianti C, Mattock H, Straif K. Carcinogenicity of FE, silicon carbide fibres and whiskers, and carbon nanotubes. Lancet Oncol. 2014;15(13):1427-8.

8. Ledda C, Loreto C, Matera S, Massimino N, Cannizzaro E, Musumeci A, Migliore M, Fenga C, Pomara C, Rapisarda V. Early effects of fluoro-edenite: Correlation between IL-18 serum levels and pleural and parenchymal abnormalities. Future Oncol. 2016;12(23s):59-62.
9. Ledda C, Rapisarda V. Malignant pleural mesothelioma: The need to move from research to clinical practice. Arch Med Res. 2016;47(5):407.
10. Ledda C, Pomara C, Bracci M, Mangano D, Ricceri V, Musumeci A, Ferrante M, Musumeci G, Loreto C, Fenga C, Santarelli L, Rapisarda V. Natural carcinogenic fiber and pleural plaques assessment in a general population: A cross-sectional study. Environ Res. 2016;150:23-9.
11. Ledda C, Loreto C, Pomara C, Rapisarda G, Fiore M, Ferrante M, Bracci M, Santarelli L, Fenga C, Rapisarda V. Sheep lymph-nodes as a biological indicator of environmental exposure to fluoro-edenite. Environ Res. 2016;147:97-101.
12. Ledda C, Costa C, Matera S, Puglisi B, Costanzo V, Bracci M, Fenga C, Rapisarda V, Loreto C. Immunomodulatory effects in workers exposed to naturally occurring asbestos fibers. Mol Med Rep. 2017;15(5):3372-8.
13. Ledda C, Caltabiano R, Loreto C, Cinà D, Senia P, Musumeci A, Ricceri V, Pomara C, Rapisarda V. Prevalence of anti-nuclear autoantibodies in subjects exposed to natural asbestiform fibers: A cross-sectional study. J Immunotoxicol. 2018;15(1):24-8. DOI: 10.1080/1547691X.2017.1415398.
14. Martinez G, Loreto C, Rapisarda V, Musumeci G, Valentino M, Carnazza ML. Effects of exposure to fluoro-edenite fibre pollution on the respiratory system: an in vivo model. Histol Histopathol. 2006;21(4-6):595-601.
15. Rapisarda V, Loreto C, Castorina S, Romano G, Garozzo SF, Musumeci A, Migliore M, Avola R, Cinà D, Pomara C, Ledda C. Occupational exposure to fluoro-edenite and prevalence of anti-nuclear autoantibodies. Future Oncol. 2018;14(6s):59-62. DOI: 10.2217/fon-2017-0389.
16. Paoletti L, Batisti D, Bruno C, Di Paola M, Gianfagna A, Mastrantonio M, Nesti M, Comba P. Unusually high incidence of malignant pleural mesothelioma in a town of eastern Sicily: an epidemiological and environmental study. Arch of Environ Heal: An Intern J. 2000;55(6):392-398.
17. Di Paola M, Mastrantonio M, Carboni M, Belli S, Grignoli M, Comba P, Nesti M. Mortality from malignant pleural neoplasms in Italy in the years 1988-1992. Rome, Ist Super di San. 1996;Rapporti ISTISAN, 96/40.
18. Fazzo L, De Santis M, Minelli G, Bruno C, Zona A, Marinaccio A, Conti S, Comba, P. Pleural mesothelioma mortality and asbestos exposure mapping in Italy. Am J Industr Med. 2011;55(1):11-24. DOI: 10.1002/ajim.21015.
19. Galateau-Salle F, Churg A, Roggli V, Travis WD. The 2015 World Health Organization classification of tumors of the pleura: advances since the 2004 classification. J Thorac Oncol. 2016;11:142–54. DOI: 10.1016/j.jtho.2015.11.005.
20. Rapisarda V, Ledda C, Ricceri V, Arena F, Musumeci A, Marconi A, Fago L, Bracci M, Santarelli L, Ferrante M. Detection of pleural plaques in workers exposed to inhalation of natural fluoro-edenite fibres. Oncol Lett. 2015;9(5):2046-52.

21. Travaglione S, Bruni B, Falzano I, Paoletti I, Fiorentini C. Effects of the new-identified amphibole fluoro-edenite in lung epithelial cells. Tox in Vitro. 2003;17(5-6):547-52.
22. Ledda C, Lombardo C, Tendi EA, Hagnäs M, Paravizzini G, Filetti V, Rapisarda V. Pathway of Inflammation due to Asbestiform Fiber “Fluoro-edenite” Exposure: An Update. Current Respiratory Medicine Reviews. 2020;16(2):73–75.
23. Loreto C, Caltabiano R, Graziano ACE, Castorina S, Lombardo C, Filetti V, Vitale E, Rapisarda G, Cardile V, Ledda C, Rapisarda V. Defense and protection mechanisms in lung exposed to asbestiform fiber: The role of macrophage migration inhibitory factor and heme oxygenase-1. European Journal of Histochemistry. 2020;64(2):95-103, 3073.
24. Yang H, Testa JR, Carbone M. Mesothelioma epidemiology, carcinogenesis, and pathogenesis. Curr Treat Options Oncol. 2008;9:147-157.
25. Micolucci L, Rippo MR, Olivieri F, Procopio AD. Progress of research on microRNAs with diagnostic value in asbestos exposure: A call for method standardization. BioScience Trends. 2017;11(1):105-109.
26. Caltabiano R, Loreto C, Vitale E, Matera S, Miozzi E, Migliore M, Angelico G, Tumino R, Ledda C, Rapisarda V. Fibulin-3 immunoexpression in malignant mesothelioma due to fluoro-edenite: A preliminary report. Future Oncol. 2018;14(6s):53-7.
27. Arnold DT, Maskell NA. Biomarkers in mesothelioma. Ann Clin Biochem. 2017;1.
28. Angelico G, Caltabiano R, Loreto C, Ieni A, Tuccari G, Ledda C, Rapisarda V. Immunohistochemical expression of aquaporin-1 in fluoro-edenite-induced malignant mesothelioma: A preliminary report. Int J Mol Sci. 2018;19(3).
29. Wu T, Zhang W, Yang G, Li H, Chen Q, Song R, Zhao L. HMGB1 overexpression as a prognostic factor for survival in cancer: A meta-analysis and systematic review. Oncotarget. 2016;7:50417–50427.
30. Loreto C, Lombardo C, Caltabiano R, Ledda C, Hagnäs M, Filetti V, Rapisarda V. An in vivo immunohistochemical study on MacroH2A.1 in lung and lymph-node tissues exposed to an asbestiform fiber. Curr Mol Med. 2020;20:653-660.
31. Chen Z, Gaudino G, Pass HI, Carbone M, Yang H. Diagnostic and prognostic biomarkers for malignant mesothelioma: An update. Transl Lung Cancer Res. 2017;6:259-269.
32. Creaney J, Sneddon S, Dick IM, Dare H, Boudville N, Musk AW, Skates SJ, Robinson BW. Comparison of the diagnostic accuracy of the MSLN gene products, mesothelin and megakaryocyte potentiating factor, as biomarkers for mesothelioma in pleural effusions and serum. Dis Markers. 2013;35:119-127.
33. Creaney J, Dick IM, Meniawy TM, Leong SL, Leon JS, Demelker Y, Segal A, Musk AW, Lee YC, Skates SJ, et al. Comparison of fibulin-3 and mesothelin as markers in malignant mesothelioma. Thorax. 2014;69:895-902.
34. Cui A, Jin XG, Zhai K, Tong ZH, Shi HZ. Diagnostic values of soluble mesothelin-related peptides for malignant pleural mesothelioma: Updated meta-analysis. BMJ Open. 2014;4(e004145).

35. Reid G. MicroRNAs in mesothelioma: From tumour suppressors and biomarkers to therapeutic targets. J Thorac Dis. 2015;7:1031-1040.
36. Falzone L, Scola L, Zanghì A, Biondi A, Di Cataldo A, Libra M, Candido S. Integrated analysis of colorectal cancer microRNA datasets: identification of microRNAs associated with tumor development. Aging (Albany NY). 2018;10(5):1000-1014. DOI: 10.18632/aging.101444.
37. Falzone L, Lupo G, La Rosa GRM, Crimi S, Anfuso CD, Salemi R, Rapisarda E, Libra M, Candido S. Identification of Novel MicroRNAs and Their Diagnostic and Prognostic Significance in Oral Cancer. Cancers (Basel). 2019;11(5):610. DOI: 10.3390/cancers11050610.
38. Micolucci L, Akhtar MM, Olivieri F, Rippo MR, Procopio AD. Diagnostic value of microRNAs in asbestos exposure and malignant mesothelioma: systematic review and qualitative meta-analysis. Oncotarget. 2016;7:58606-58637.
39. Filetti V, Falzone L, Rapisarda V, Caltabiano R, Graziano ACE, Ledda C, Loreto C. Modulation of microRNA expression levels after naturally occurring asbestiform fibers exposure as a diagnostic biomarker of mesothelial neoplastic transformation. Ecotoxicology and Environmental Safety. 2020;198(110640). DOI: 10.1016/j.ecoenv.2020.110640.
40. Cavallari I, Urso L, Sharova E, Pasello G, Ciminale V. Liquid biopsy in malignant pleural mesothelioma: state of the art, pitfalls, and perspectives. Front Oncol. 2019;9.
41. Sato H, Soh J, Aoe K, Fujimoto N, Tanaka S, Namba K, Torigoe H, Shien K, Yamamoto H, Tomida S, Tao H, Okabe K, Kishimoto T, Toyooka S. Droplet digital PCR as a novel system for the detection of microRNA-34b/c methylation in circulating DNA in malignant pleural mesothelioma. Int. J. Oncol. 2019;54 (6):2139–2148.
42. Tuaeva NO, Falzone L, Porozov YB, Nosyrev AE, Trukhan VM, Kovatsi L, Spandidos DA, Drakoulis N, Kalogeraki A, Mamoulakis C, Tzanakakis G, Libra M, Tsatsakis A. Translational application of circulating DNA in oncology: review of the last decades achievements. Cells. 2019;8(10), E1251 pii.
43. Tomasetti M, Amati M, Neuzil J, Santarelli L. Circulating epigenetic biomarkers in lung malignancies. From early diagnosis to therapy. Lung Canc. 2017;107:65–72.
44. Ledda C, Senia P, Rapisarda V. Biomarkers for Early Diagnosis and Prognosis of Malignant Pleural Mesothelioma: The Quest Goes on. Cancers. 2018;10(6):203.
45. Crimi S, Falzone L, Gattuso G, Grillo CM, Candido S, Bianchi A, Libra M. Droplet Digital PCR Analysis of Liquid Biopsy Samples Unveils the Diagnostic Role of hsa-miR-133a-3p and hsa-miR-375-3p in Oral Cancer. Biology (Basel). 2020;9(11):379.
46. Salemi R, Falzone L, Madonna G, Polesel J, Cinà D, Mallardo D, Ascierto PA, Libra M, Candido S. MMP-9 as a Candidate Marker of Response to BRAF Inhibitors in Melanoma Patients with BRAFV600E Mutation Detected in Circulating-Free DNA. Front. Pharmacol. 2018;9(856). DOI: 10.3389/fphar.2018.00856.
47. Shirdel EA, Xie W, Mak TW, Jurisica I. NAViGaTing the micronome--using multiple microRNA prediction databases to identify signalling pathway-associated microRNAs. PLoS One. 2011;6(e17429). https://doi.org/10.1371/journal.pone.0017429

48. Tokar T, Pastrello C, Rossos AE, Abovsky M, Hauschild AC, Tsay M, Lu R, Jurisica I. mirDIP 4.1-integrative database of human microRNA target predictions. Nucleic Acids Res. 2018;46(D360–70). https://doi.org/10.1093/nar/gkx1144

49. Goldman M, Craft B, Hastie M, Repe˘cka K, McDade F, Kamath A, Banerjee A, Luo Y, Rogers D, Brooks AN, et al. Visualizing and interpreting cancer genomics data via the Xena platform. Nat Biotechnol. 2020;38:675–678.

Figures

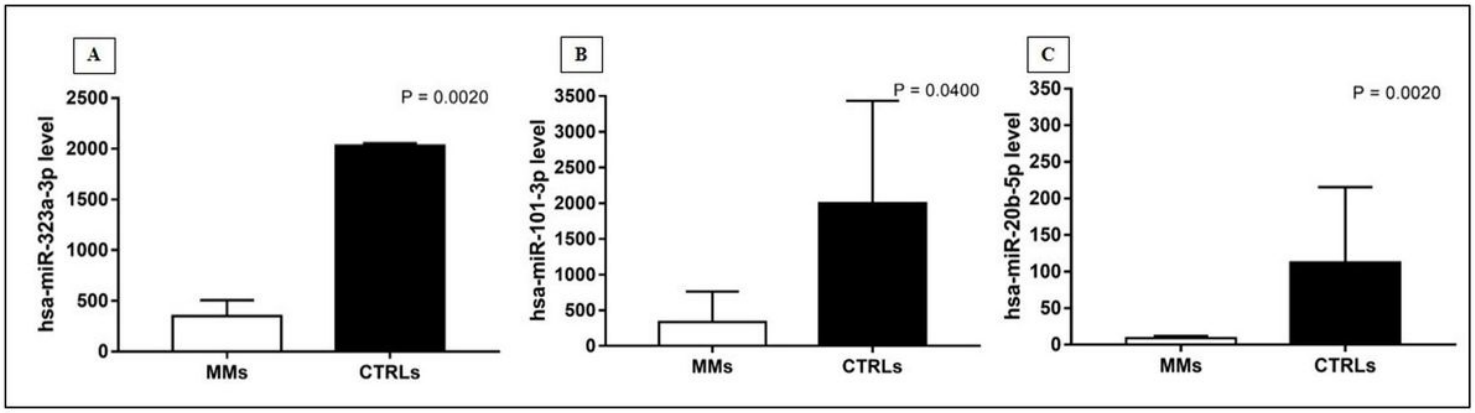

Figure 1

MiRNAs expression, reported as number of copies, in MM cases and healthy controls according to: A) hsa-miR-323a-3p; B) hsa-miR-101-3p; C) hsa-miR-20b-5p.

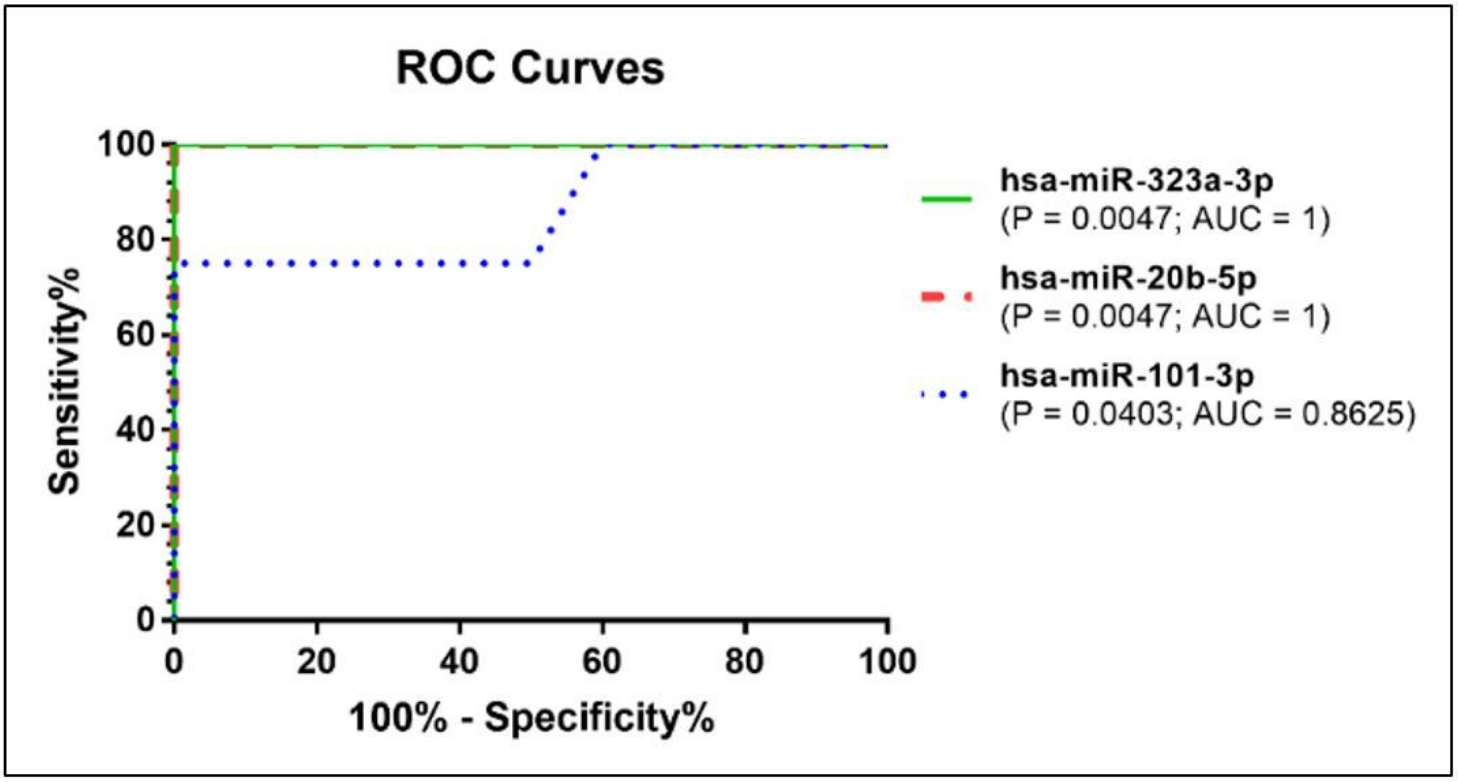

Figure 2

ROC curves demonstrated the diagnostic value of hsa-miR-323a-3p (100% Sensitivity and 100% Specificity), hsa-miR-20b-5p (100% Sensitivity and 100% Specificity), and hsa-miR-101-3p (100% Sensitivity and 40% Specificity).

Top 20 genes	miRNAs	Intensity of interaction		Medium	High	Very High
BAP1	hsa-miR-323a-3p	Medium	hsa-miR-323a-3p	50%	30%	20%
BAP1	hsa-miR-101-3p	Medium	hsa-miR-101-3p	45%	25%	30%
BAP1	hsa-miR-20b-5p	Medium	hsa-miR-20b-5p	15%	45%	40%
NF2	hsa-miR-323a-3p	Medium				
NF2	hsa-miR-101-3p	Medium				
NF2	hsa-miR-20b-5p	High				
TP53	hsa-miR-323a-3p	Medium				
TP53	hsa-miR-101-3p	Medium				
TP53	hsa-miR-20b-5p	High				
SETD2	hsa-miR-323a-3p	High				
SETD2	hsa-miR-101-3p	High				
SETD2	hsa-miR-20b-5p	Very High				
LATS2	hsa-miR-323a-3p	High				
LATS2	hsa-miR-101-3p	Medium				
LATS2	hsa-miR-20b-5p	High				
FBXW7	hsa-miR-323a-3p	Medium				
FBXW7	hsa-miR-101-3p	Very High				
FBXW7	hsa-miR-20b-5p	Very High				
DDX3X	hsa-miR-323a-3p	Very High				
DDX3X	hsa-miR-101-3p	Very High				
DDX3X	hsa-miR-20b-5p	High				
EGFR	hsa-miR-323a-3p	Medium				
EGFR	hsa-miR-101-3p	High				
EGFR	hsa-miR-20b-5p	Very High				
SF3B1	hsa-miR-323a-3p	High				
SF3B1	hsa-miR-101-3p	High				
SF3B1	hsa-miR-20b-5p	Medium				
PBRM1	hsa-miR-323a-3p	Very High				
PBRM1	hsa-miR-101-3p	Very High				
PBRM1	hsa-miR-20b-5p	Very High				
KRAS	hsa-miR-323a-3p	Very High				
KRAS	hsa-miR-101-3p	High				
KRAS	hsa-miR-20b-5p	Very High				
PIK3CA	hsa-miR-323a-3p	High				
PIK3CA	hsa-miR-101-3p	Medium				
PIK3CA	hsa-miR-20b-5p	High				
CTNNB1	hsa-miR-323a-3p	Medium				
CTNNB1	hsa-miR-101-3p	High				
CTNNB1	hsa-miR-20b-5p	High				
CREBBP	hsa-miR-323a-3p	High				
CREBBP	hsa-miR-101-3p	Medium				
CREBBP	hsa-miR-20b-5p	High				
NSD1	hsa-miR-323a-3p	Medium				
NSD1	hsa-miR-101-3p	Very High				
NSD1	hsa-miR-20b-5p	High				
ZFHX3	hsa-miR-323a-3p	Very High				
ZFHX3	hsa-miR-101-3p	Very High				
ZFHX3	hsa-miR-20b-5p	Very High				
APC	hsa-miR-323a-3p	Medium				
APC	hsa-miR-101-3p	Very High				
APC	hsa-miR-20b-5p	Very High				
LATS1	hsa-miR-323a-3p	Medium				
LATS1	hsa-miR-101-3p	Medium				
LATS1	hsa-miR-20b-5p	High				
LRP1B	hsa-miR-323a-3p	High				
LRP1B	hsa-miR-101-3p	Medium				
LRP1B	hsa-miR-20b-5p	Very High				
BRAF	hsa-miR-323a-3p	Medium				
BRAF	hsa-miR-101-3p	Medium				
BRAF	hsa-miR-20b-5p	Medium				

Figure 3

Interaction between selected miRNAs and main altered genes in MM by mirDIP gene target analysis. For each miRNA the level of interaction with the 20 genes involved in MM is reported. The intensity of interaction is highlighted with a color scale ranging from yellow (medium interaction) to red (very high interaction).

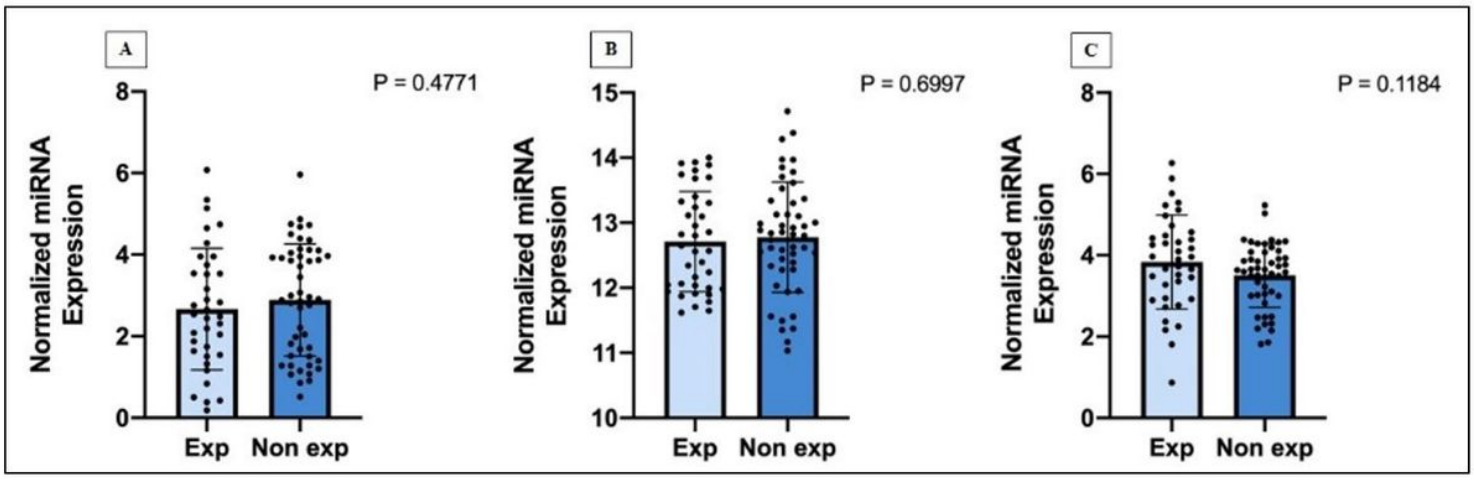

Figure 4

Normalized miRNAs expression in MM cases exposed and non exposed to asbestos according to: A) hsa-miR-323a-3p; B) hsa-miR-101-3p; C) hsa-miR-20b-5p.

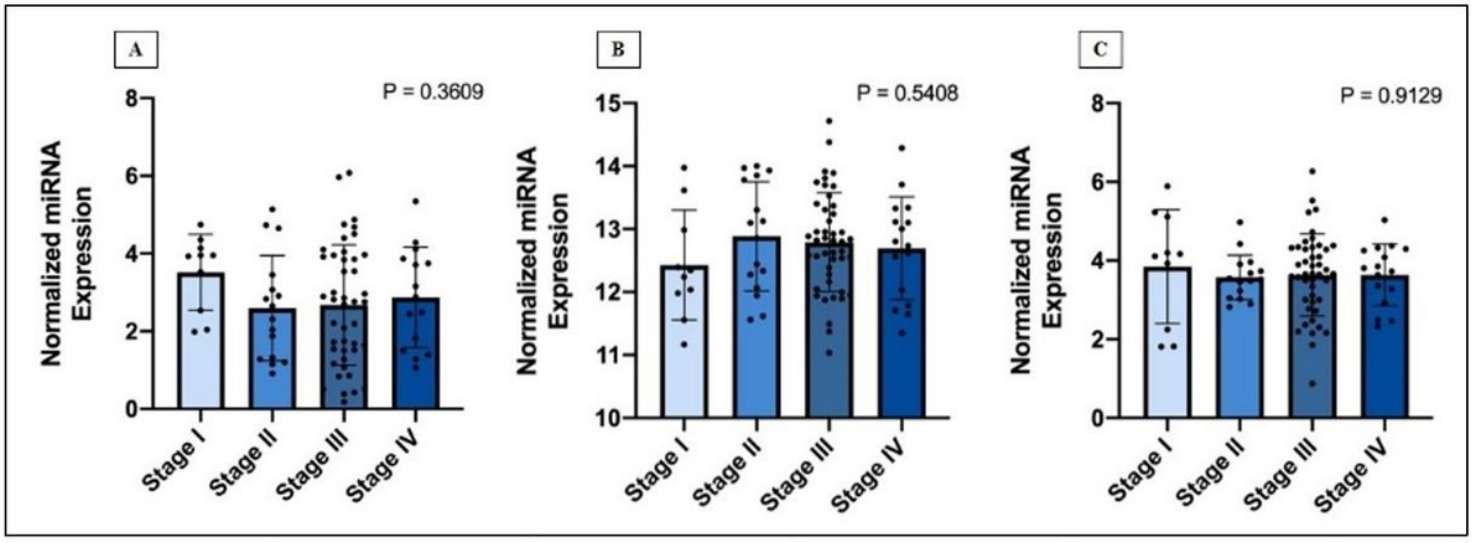

Figure 5

Normalized miRNAs expression in different MM stages according to: A) hsa-miR-323a-3p; B) hsa-miR-101-3p; C) hsa-miR-20b-5p.

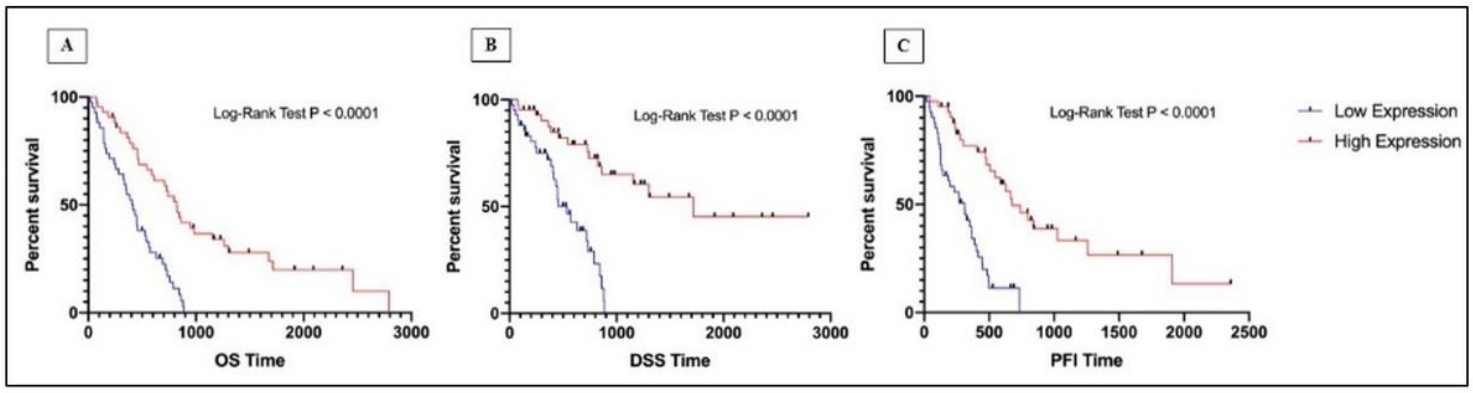

Figure 6

Kaplan-Meier survival curve of hsa-miR-101-3p expression in MM patients according to: A) OS Time; B) DSS Time; C) PFI Time.